Juxtaposition of the changes in intracellular calcium and force during staircase potentiation at 30 and 37°C

Ian C. Smith,[1] Rene Vandenboom,[2] and A. Russell Tupling[1]

[1]Department of Kinesiology, University of Waterloo, Waterloo, Ontario N2L 3G1, Canada
[2]Department of Kinesiology, Brock University, St. Catharines, Ontario L2S 3A1, Canada

Ca^{2+} entry during the action potential stimulates muscle contraction. During repetitive low frequency stimulation, skeletal muscle undergoes staircase potentiation (SP), a progressive increase in the peak twitch force induced by each successive stimulus. Multiple mechanisms, including myosin regulatory light chain phosphorylation, likely contribute to SP, a temperature-dependent process. Here, we used the Ca^{2+}-sensitive fluorescence indicators acetoxymethyl (AM)-furaptra and AM-fura-2 to examine the intracellular Ca^{2+} transient (ICT) and the baseline Ca^{2+} level at the onset of each ICT during SP at 30 and 37°C in mouse lumbrical muscle. The stimulation protocol, 8 Hz for 8 s, resulted in a $27 \pm 3\%$ increase in twitch force at 37°C and a $7 \pm 2\%$ decrease in twitch force at 30°C ($P < 0.05$). Regardless of temperature, the peak rate of force production ($+df/dt$) was higher in all twitches relative to the first twitch ($P < 0.05$). Consistent with the differential effects of stimulation on twitch force at the two temperatures, raw ICT amplitude decreased during repetitive stimulation at 30°C ($P < 0.05$) but not at 37°C. Cytosolic Ca^{2+} accumulated during SP such that baseline Ca^{2+} at the onset of ICTs occurring late in the train was higher ($P < 0.05$) than that of those occurring early in the train. ICT duration increased progressively at both temperatures. This effect was not entirely proportional to the changes in twitch duration, as twitch duration characteristically decreased before increasing late in the protocol. This is the first study identifying a changing ICT as an important, and temperature-sensitive, modulator of muscle force during repetitive stimulation. Moreover, we extend previous observations by demonstrating that contraction-induced increases in baseline Ca^{2+} coincide with greater $+df/dt$ but not necessarily with higher twitch force.

INTRODUCTION

Excitation–contraction coupling is the process by which depolarization of the muscle membrane is converted into mechanical forces by striated muscle cells. The voltage-gated release of Ca^{2+} from the terminal cisternae of the SR produces transient elevations in cytosolic Ca^{2+} levels that regulate several processes including muscle force. Ca^{2+} binding to troponin C relieves stearic hindrances to cross-bridge formation, i.e., formation of the strongly bound actomyosin complex on the thin filament, and thus allows force production. Cytosolic Ca^{2+} concentration is returned to basal levels by the sarco-endoplasmic reticulum Ca^{2+}-ATPase (SERCA), an ATP-dependent pump that translocates Ca^{2+} across the SR membrane. Although a single action potential produces only a "twitch," repeated action potentials yielding more sustained elevations in Ca^{2+} produce a "tetanus" with much greater force-time integral output of striated muscle contraction.

The twitch force produced by a muscle is extremely history dependent and is thus highly labile. As an example, repetitive stimulation of fast-twitch skeletal muscle at low stimulation frequencies (<10 Hz) produces a stepwise or progressive increase in twitch force to a new peak (Isaacson, 1969), known as staircase potentiation (SP). The magnitude of SP is dependent on several factors including temperature, being reduced as muscle cools (Walker, 1951; Close and Hoh, 1968; Hanson, 1974; Krarup, 1981; Moore et al., 1990; Vandenboom et al., 2013). Based on the characteristics of the action potential measured during brief but repetitive stimulation of rat intercostal skeletal muscle (in vitro) at 22 and 37°C (Hanson, 1974), the temperature dependence for SP likely originates downstream of membrane excitability and voltage-gated Ca^{2+} release channel open probability per se (Vandenboom et al., 2013).

The primary intracellular mechanism for SP may be posttranslational modifications of the myosin motor molecule concomitant with repetitive stimulation of fast-twitch skeletal muscle. As an example, repetitive stimulation of rodent fast-twitch skeletal muscle has been

demonstrated to increase the phosphate content of the myosin regulatory light chain (RLC) subunits (Klug et al., 1982; Manning and Stull, 1982), a reaction that increases the Ca^{2+} sensitivity, but not maximal force, of permeabilized skeletal fibers (Persechini et al., 1985; Metzger et al., 1989). These studies thus provide a mechanistic explanation for the ability of repetitive stimulation to enhance twitch without influencing tetanic force (Sweeney and Stull, 1990). A small but growing body of evidence, however, suggests the existence of multiple or complementary mechanisms for SP. For example, extensor digitorum longus (EDL) muscles devoid of skeletal myosin light chain kinase, the enzyme responsible for phosphorylating the RLC, exhibit SP in the absence of RLC phosphate incorporation (Zhi et al., 2005; Gittings et al., 2011). Moreover, denervated rat gastrocnemius muscles displaying reduced levels of RLC phosphorylation retain SP (Rassier et al., 1999; MacIntosh et al., 2008). Although an alternative mechanism has not definitively been identified, our recent work has shown that posttetanic potentiation (PTP) of the mouse lumbrical, a muscle without detectable RLC phosphorylation, is associated with elevations in cytosolic Ca^{2+} immediately before the onset of an intracellular Ca^{2+} transient (ICT), such that baseline Ca^{2+} is higher at the onset of potentiated contractions than unpotentiated contractions (Smith et al., 2013). However, it remains to be determined if changes in the ICT and/or baseline Ca^{2+} at the onset of the ICT contribute to SP in the mouse lumbrical.

The primary purpose of this investigation was to compare and contrast the changes in force with the changes in the cytosolic Ca^{2+} during SP at two different temperatures (i.e., 30 and 37°C) to determine if stimulation-induced changes in either the ICTs or the baseline Ca^{2+} level at the onset of each ICT could contribute to the SP response. To this end, we measured the changes in the isometric twitch force in mouse lumbrical muscles after loading with Ca^{2+}-sensitive fluorescence indicators, either acetoxymethyl (AM)-furaptra or AM-fura-2, which were, respectively, used to monitor changes in the ICT and baseline Ca^{2+}. We hypothesized that there would be temperature-dependent declines in the amplitude and area of the Ca^{2+}-time integral of the ICT, which may help account for the reduced potentiation seen at low versus high temperatures. We hypothesized that just as in PTP (Smith et al., 2013), baseline Ca^{2+} would be elevated at the onset of twitches exhibiting SP, regardless of temperature.

MATERIALS AND METHODS

All methods used in this study were approved by the University of Waterloo Animal Care Committee, and all experiments were performed in the laboratory of A.R. Tupling at the University of Waterloo. Detailed descriptions of the methods used in this study were reported recently (Smith et al., 2013). In brief, after sacrifice by cervical dislocation, the lumbrical muscles from the hind feet of 3–6-mo-old male C57BL/6 mice were excised in Tyrode's dissecting solution (mM: 136.5 NaCl, 5.0 KCl, 11.9 NaHCO$_3$, 1.8 CaCl$_2$, 0.40 NaH$_2$PO$_4$, 0.10 EDTA, and 0.50 MgCl$_2$, pH 7.5; on ice). Muscles were then suspended at optimum length for twitch-force
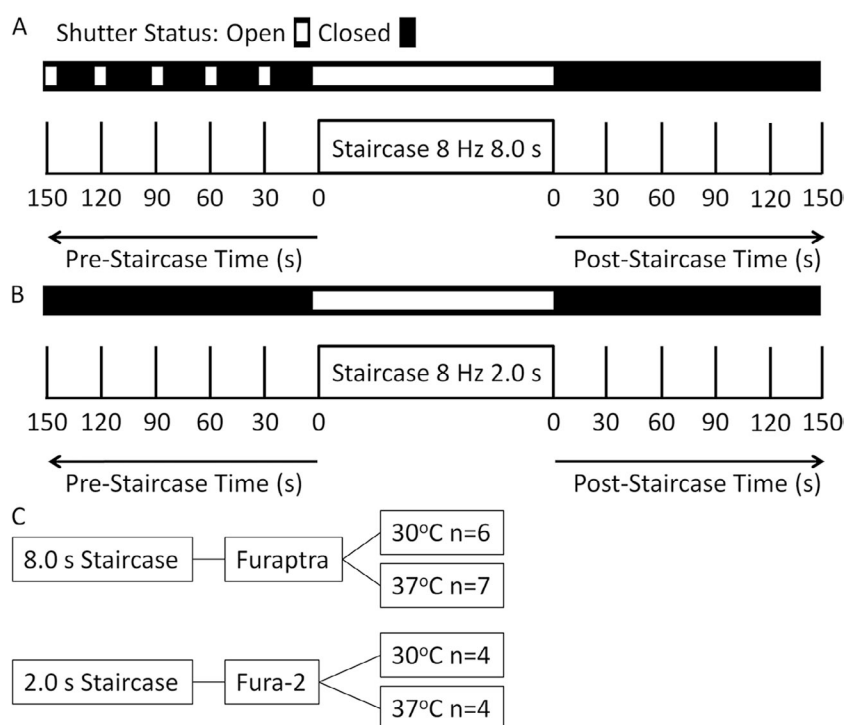
Figure 1. SP experimental time line and schematic. Isolated mouse lumbricals loaded with either AM-furaptra or AM-fura-2 were stimulated at 30-s intervals before an 8-Hz volley to elicit SP, after which twitch contractions were resumed at 30-s intervals to monitor the dissipation of the potentiation response. Muscles loaded with furaptra were subject to the protocol depicted in A. Here, the shutter controlling exposure to light was open for 1-s windows during individual twitch contractions and for 9-s windows during 8 s of 8-Hz contraction. Muscles loaded with fura-2 were subjected to the protocol depicted in B. Here, because of photo-bleaching concerns, the 8-Hz contraction was limited to 2 s and the shutter was opened for 3 s. No fluorescence measurements were made during the single twitches preceding the 8-Hz stimulation. These procedures were repeated 10 times for each muscle with 30–60-s gaps between consecutive trials. The wavelength of light used to excite the fluorescence indicators was alternated between 344 and 380 nm, one wavelength per trial, producing five ratio signals (380/344 nm) per twitch per muscle. Schematic diagrams demonstrate the experimental design and n values used for each indicator and temperature (C).

production (L_o) between a high speed length controller (model 322C; Aurora Scientific Inc.) and a force transducer (model 400A; Aurora Scientific Inc.) in a bath containing circulating oxygenated (95% O_2, 5% CO_2) Tyrode's experimental solution (mM: 121.0 NaCl, 5.0 KCl, 24.0 NaHCO$_3$, 1.8 CaCl$_2$, 0.40 NaH$_2$PO$_4$, 5.50 glucose, 0.10 EDTA, and 0.50 MgCl$_2$, pH 7.3) at either 30 or 37°C. Stimulation was applied through flanking platinum plate field stimulus electrodes using a stimulator (model 701C; Aurora Scientific Inc.) at supramaximal voltage. Lumbrical muscles were loaded with the low affinity ratiometric Ca^{2+} indicator AM-furaptra (Molecular Probes) to detect transient changes in the intracellular Ca^{2+} concentration. Separate muscles were loaded with the high affinity, ratiometric Ca^{2+} indicator AM-fura-2 to monitor changes in baseline Ca^{2+}. Monochromator-controlled light (Photon Technology International) at either 380 or 344 nm provided the excitation signal to the muscle-bound indicators, and the resulting 510-nm fluorescence emission signals were collected through an inverted microscope photometer system (D-104; Photon Technology International) affixed with a photomultiplier tube (model 814; Photon Technology International). Analogue force and fluorescence signals were digitized and collected at 10,000 Hz and stored for later analysis.

Experimental protocol

A schematic illustration of the stimulation protocols used in this study is shown in Fig. 1 (A and C). AM-furaptra–loaded lumbricals were stimulated once per 30 s to produce a steady isometric twitch-force response. Fluorescence emission signals from the last six twitches were used to determine the characteristics of the unpotentiated ICT. This pacing procedure was then halted, and an 8-Hz stimulation protocol lasting for 8 s was initiated with continuous fluorescence emission monitoring. This protocol was used as it allowed force to return to resting values between consecutive twitches at both 30 and 37°C. The muscle was then subjected to the pacing protocol for 5 min to monitor dissipation of the potentiation response. The excitation wavelength was adjusted and the stimulation protocol was repeated 10 times per muscle, alternating between 380- and 344-nm excitation to produce five fluorescence ratio signals, which were averaged together during data analysis. Data were further condensed by averaging the five unpotentiated

twitches into a single record, whereas the 8-Hz stimulation data were condensed into four windows where all twitches within 2-s blocks were averaged together, i.e., 16 twitches per window. Muscles generally tolerated this protocol well, as tetanic force did not change over the course of the protocol. Twitch force, however, declined between the first and 10th trials. There was a trend toward greater reduction of twitch force at 37°C than at 30°C (30°C: 16 ± 3% vs. 37°C: 23 ± 5%; P = 0.14), in contrast to the greater reduction in ICT amplitude seen at 30°C compared with 37°C. This suggests that even if a systematic decline in Ca^{2+} release occurs, it should not affect our conclusions. Furthermore, the early decline in ICT amplitude seen during SP, the lack of a difference in ICT characteristics during PTP (Smith et al., 2013), and the return of twitch force to prestimulation levels within 30 s of recovery all suggest fast recovery of ICT amplitude after cessation of repetitive stimulation. At 37°C, potentiation systematically increased between the first and 10th trials, and at 30°C, force depression systematically decreased (final force was relatively higher in later trials, although it never achieved potentiation). Both ICT signals and force data were averaged across the 10 repetitions. Thus, all data reflect the average response of the 10 trials for each muscle, which should control for any systematic decline in twitch force (and Ca^{2+} release or sensitivity).

To gain greater insight into the changes in the ICT during the first 2 s of SP, a second analysis of the furaptra recordings was performed using finer groupings, specifically the combination of twitches 1–6, 6–11, and 11–16 in the SP protocol. Asynchronous measurement of emission signals is a salient feature of dual-excitation mono-emission ratioable indicators, which leaves room for signal contamination by motion artifact. For example, small changes in the contraction between consecutive trials may result in varying amounts of indicator in the field of view; thus, it cannot be said that our measurements are entirely free of motion artifact. However, extensive testing has verified the effectiveness of our protocols to cancel the motion during sinusoidal length changes (Smith, 2014; see also Morgan et al., 1997). Additionally, we have carefully checked the data for any large mismatches in the emission signals, and in the hundreds of repetitions, we found only one instance of mismatch with significant consequence on the resultant ratio, which was subsequently removed from the data.
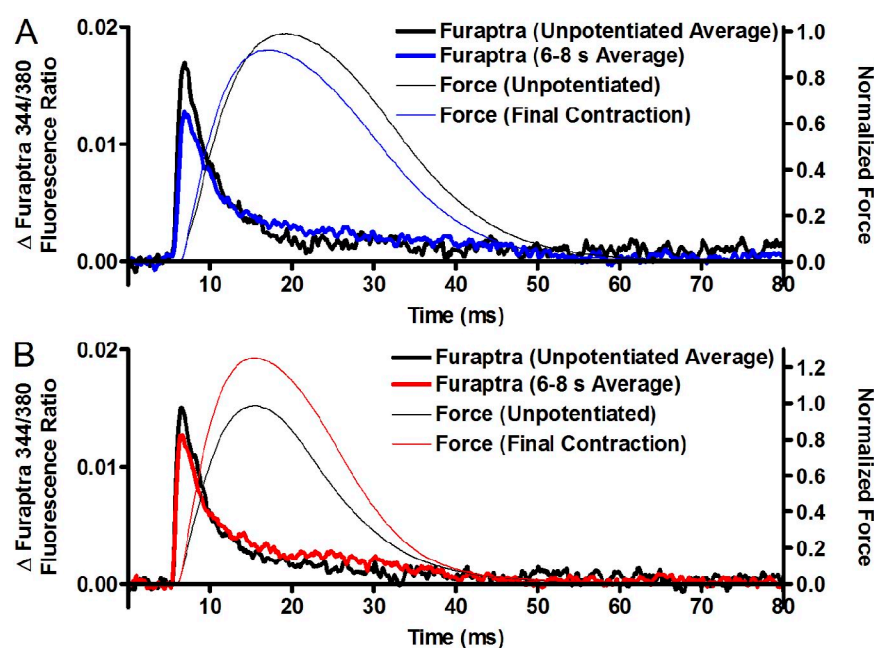
Figure 2. Representative force and furaptra tracings during 8-Hz stimulation. The force recordings, taken at either 30 ($n = 6$; A) or 37°C ($n = 7$; B) correspond to the first (unpotentiated) and final contractions during the protocol. Furaptra recordings are the average of either six averaged records taken at 30-s intervals before the 8-Hz stimulation protocol (unpotentiated), or 16 averaged records over the final 2 s of the stimulation protocol, with each averaged record resulting from 10 repetitions of the protocol depicted in Fig. 1. Values are expressed relative to the average ratio over the 10 ms immediately preceding each contraction.

Thus, we are confident that the signals presented are a good representation of the changes in cellular Ca^{2+}.

Western blotting

An additional component of this study was to characterize the expression of the muscle relaxation enzymes (SERCA1a, SERCA2a, and parvalbumin) in whole muscle homogenates of the lumbrical, soleus, and EDL of the mouse using Western blotting techniques ($n = 8$). Separation of proteins was performed by electrophoresis using either 7.5% polyacrylamide glycine gels (SERCA1a and SERCA2a) or 13% polyacrylamide tricine gels (parvalbumin) and standard SDS/PAGE protocols (Laemmli, 1970). Protein concentrations of homogenates were determined by the bicinchoninic acid method (Sigma-Aldrich) and verified using Ponceau S (BioShop Canada Inc.). A linear relationship between band density and protein load was established for each mouse using either EDL (SERCA1a and parvalbumin) or soleus (SERCA2a) to form a scale, against which the other muscles were compared. After semi-dry transfer of proteins to polyvinyl difluoride membranes, primary probing was performed using monoclonal anti-SERCA1a A52 (provided by D. MacLennan, University of Toronto, Toronto, Canada), anti-SERCA2a 2A7-A1 (Thermo Fisher Scientific), and PVG 214 goat anti-parvalbumin (Swant). Secondary probing was performed using goat anti–mouse (SERCA1a and SERCA2a; Santa Cruz Biotechnology, Inc.) or donkey anti–goat (parvalbumin; Santa Cruz Biotechnology, Inc.). Detection was performed using a Luminata HRP substrate detection kit (EMD Millipore), and subsequent quantification was based on densitometric analysis obtained using GeneSnap and GeneTools software (GE Healthcare).
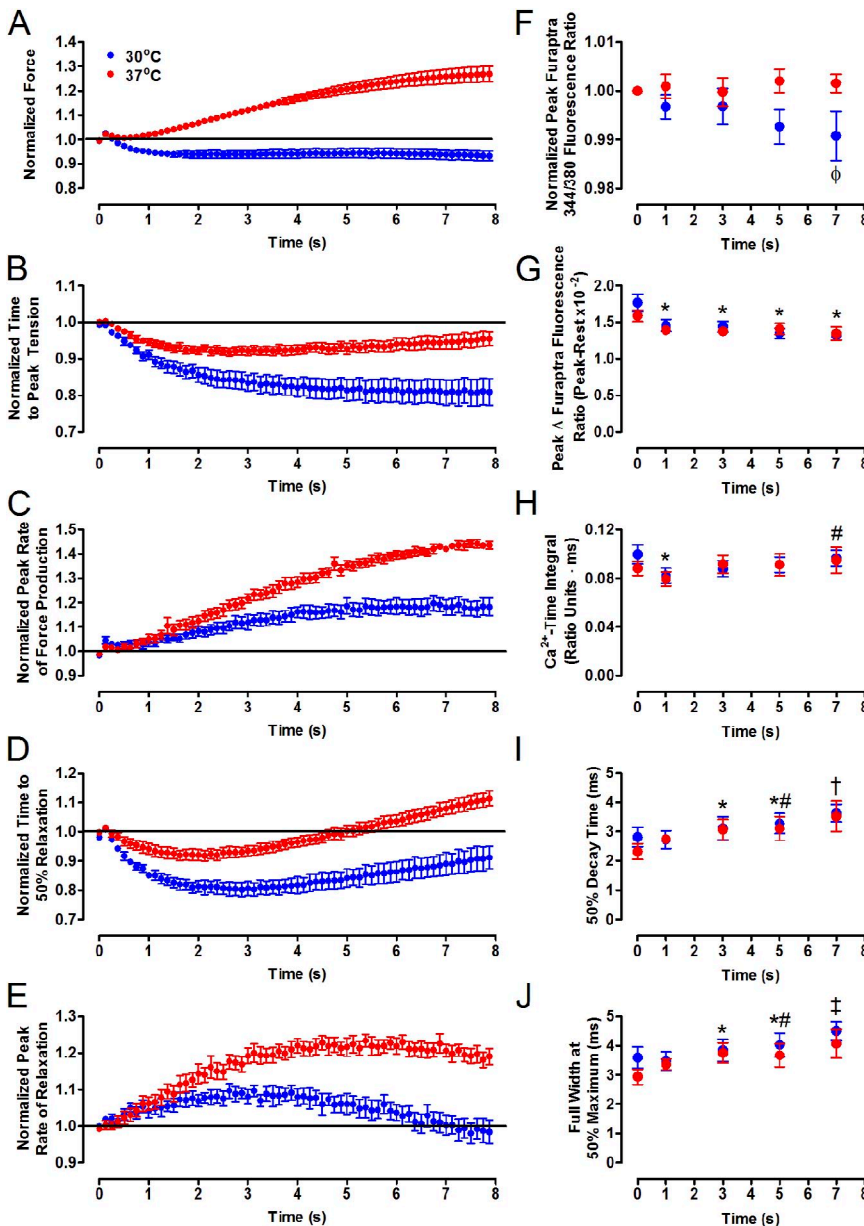
Figure 3. Twitch and ICT characteristics during 8-Hz stimulation. Mouse lumbrical muscles loaded with AM-furaptra were subjected to 10 cycles of 8-Hz stimulation for 8 s separated by 5 min during which the muscles were stimulated once every 30 s. Experiments were performed at either 30 ($n = 6$; blue) or 37°C ($n = 7$; red). Peak force (A), TPT (B), $+df/dt$ (C), $1/2RT$ (D), and $-df/dt$ (E) were all normalized to the average of the three twitches immediately preceding the onset of the 8-Hz stimulation protocol for each temperature. Data were averaged across the 10 trials for each muscle. Furaptra recordings during 8-Hz stimulation are averaged over 2-s intervals and plotted in the center of these intervals (i.e., 1, 3, 5, and 7 s), whereas recordings for control twitches were measured at 30-s intervals (the average of six records) before the onset of the staircase protocol and are plotted at time 0. The peak amplitudes of the resultant the furaptra recordings are presented relative to the initial ratio values for each temperature (F). Furaptra records were then adjusted to a baseline defined as the average ratio over the 10 ms immediately before each stimulus, and data presented in G–J were calculated from these records. The peak Δ furaptra ratio (G) represents the difference between the maximum ratio during the ICT and the baseline ratio. Ca^{2+}-time integrals represent the area confined by the baseline ratio and the transient ratio, lasting 20 ms after the stimulation (H). 50% decay time (I) refers to the Ca^{2+}-removal phase of the ICT and is defined as the time it takes the signal to decline from the peak Δ furaptra ratio to 50% of this value. Similarly, the full width at 50% maximum is the duration of the ICT at 50% of the peak Δ furaptra ratio (J). All values are mean ± SEM. Φ, 30°C value is different from 0-s value at 30°C; *, main effect of repeated stimulation (values are different from the 0-s time point independent of temperature); #, main effect of repeated stimulation (values are different from the 1-s time point independent of temperature); †, main effect of repeated stimulation (values are different from 0, 1, and 3 s independent of temperature); ‡, main effect of repeated stimulation (values are different from 0, 1, 3, and 5 s independent of temperature); $P < 0.05$ for all.

Condition	Force			Potentiation
	mN			*%*
Twitch number	90 s Pre	1	64	64
30°C	22.7 ± 1.8	22.5 ± 1.7	21.0 ± 1.6[a]	−6.8 ± 1.9
37°C	17.4 ± 1.7[b]	17.3 ± 1.7[b]	21.7 ± 1.8[a]	26.8 ± 3.2[b]

Mouse lumbrical muscles were stimulated at 8 Hz for 8 s at either 30 or 37°C. Peak twitch force is reported for the first (Twitch 1) and last twitches (Twitch 64) of this protocol, along with an unpotentiated twitch occurring 90 s before the initiation of the stimulation protocol (90 s Pre). Percent potentiation refers to the relative change in peak force seen between the first and last twitches within each condition. See Figs. 2 and 3 for more detailed results. All values are presented as mean ± SEM.
[a]Different from twitch 1 and 90 s Pre ($P < 0.05$).
[b]Different than 30°C ($P < 0.05$).

Statistics

All data are reported as mean ± SEM. Relative changes in mean values for various twitch-force and Ca^{2+} parameters were compared by two-way split-plot ANOVA as appropriate using temperature (between groups) and time (repeated measures), followed by Tukey's honestly significant difference post-hoc analysis using Statistica 7 software. Differences were considered significant at $P < 0.05$.
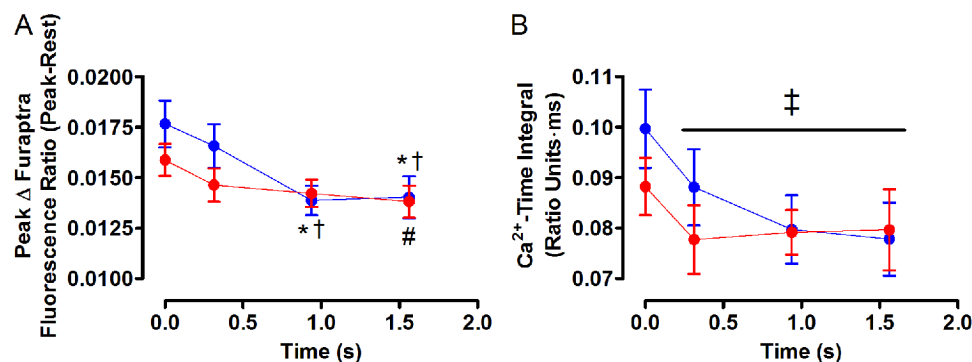
RESULTS

Force response

Representative force tracings and corresponding ICT measurements from the 8-s stimulation protocol are shown in Fig. 2, whereas the mean data are presented in Fig. 3. Consistent with previous reports (Krarup, 1981; Zhi et al., 2005; Ryder et al., 2007), the force and kinetic responses were complex as the first 1–2 s were marked by declining force and accelerating twitch-time course at both temperatures. The results from this initial period are reported in greater detail below. Beyond ∼2 s,

twitch force, the time to peak tension (TPT), and time to 50% relaxation (1/2RT) progressively increased at 37°C, whereas at 30°C, force remained relatively stable at a depressed level, TPT declined slowly, and the 1/2RT progressively increased. The changes in the peak rate of force production ($+df/dt$) exhibited a similar pattern to the changes in twitch force at 37°C. Interestingly, $+df/dt$ was consistently elevated during the stimulation protocol at 30°C, but this change did not track with the changes in peak twitch force at this temperature. The peak rate of relaxation ($-df/dt$) initially increased at both temperatures, before reaching a plateau and finally declining in the final seconds of the protocol (Fig. 3 E). Overall, at 37°C, 8 s of 8-Hz stimulation resulted in a twitch with 26.8 ± 3.2% higher force, 4.4 ± 1.9% lower TPT, 11.4 ± 2.5% higher 1/2RT, 43.6 ± 1.6% faster $+df/dt$, and 11.1 ± 2.5% faster $-df/dt$ than an unpotentiated twitch (all $P < 0.05$; see representative tracings in Fig. 2 A and raw force values in Table 1). In comparison, at 30°C, 8 s of 8-Hz stimulation resulted in a final twitch with 6.8 ± 2.0% lower force ($P < 0.05$), 19.0 ± 3.7% lower TPT ($P < 0.05$), 8.8 ± 3.9% lower 1/2RT ($P < 0.05$), 18.3 ± 3.6% faster $+df/dt$ ($P < 0.05$), and 1.6 ± 3.2% slower $-df/dt$ (not significant) than an unpotentiated twitch. Interestingly, 30 s after the stimulation protocol, the differences in the kinetic characteristics of the twitches at 30 and 37°C became quite similar, with both temperatures exhibiting potentiated force (3.4 ± 1.1 and 7.4 ± 2.4% relative to unpotentiated levels at 30 and 37°C, respectively), whereas $-df/dt$ was faster and 1/2RT was reduced relative to unpotentiated twitches (all $P < 0.05$; not depicted).

Furaptra recordings

Fluorescence ratio signals from lumbricals loaded with AM-furaptra were averaged together in 2-s windows during the 8-Hz stimulation protocol and across six unpotentiated twitches occurring at 30-s intervals before


Figure 4. ICT characteristics during the first 2 s of 8-Hz stimulation. Isolated mouse lumbrical muscles loaded with AM-furaptra were subjected to 8 s of 8-Hz stimulation, as described in Materials and methods. Resultant fluorescence ratio signals from the first 2 s were analyzed using finer groupings of twitches than those used in Fig. 3. Specifically, these groupings consisted of twitches 1–6, 6–11, and 11–16 inclusively, and are plotted in the center of the time intervals. The grouping of unpotentiated ICT values are unchanged from the analysis used in Fig. 3, and are plotted at time point 0. The changes in ICT amplitude (A) and Ca^{2+}-time integral (B) are shown. *, interaction effect: the 30°C unpotentiated values are different than the 30°C 6–11 and the 30°C 11–16 grouping values; †, interaction effect: the 30°C 6–11 and the 30°C 11–16 grouping values are different than the 30°C 1–6 grouping values ($P < 0.05$); #, interaction effect: the 37°C 11–16 grouping values are different than the 37°C unpotentiated values ($P < 0.05$); ‡, main effect: the 1–6, 6–11, and 11–16 are all less than unpotentiated values independent of temperature.

initiating the 8-Hz stimulation. Relative changes in the peak amplitude of the resultant ratio signals are presented in Fig. 3 F. The peak amplitude significantly declined ($P < 0.05$) by the end of the protocol at 30°C, whereas peak amplitude was maintained at 37°C. The raw furaptra ratio records were next adjusted to eliminate the differences in the baseline fluorescence ratio at the onset of each stimulus. The resultant records were averaged together as above. Analysis of these records revealed that regardless of temperature, peak change in amplitude was lower during the 8-Hz stimulation protocol relative to the unpotentiated ICT (Fig. 3 G). The decline in peak amplitude was reflected by a decline in the Ca^{2+} time integral during the first 2 s of staircase ($P < 0.05$); however, the Ca^{2+}-time integral was no longer significantly different than initial unpotentiated

values by beyond 2–4 s, and was significantly greater than 0–2 s at 6–8 s (Fig. 3 H). As the time-dependent increase in the Ca^{2+}-time integral was absent if the integration time was reduced from 20 to 10 ms (not depicted), this particular effect can be attributed to increases in the decay time of the ICT. Consistent with this attribution were the progressive elevations in 1/2RT and full width at half-maximum (Fig. 3, I and J). Although these were all temperature-independent effects, the magnitudes of the initial decreases in the peak ratios (30°C $3.13 \times 10^{-3} \pm 0.44 \times 10^{-3}$ vs. 37°C $1.68 \times 10^{-3} \pm 0.44 \times 10^{-3}$ ratio units; $P < 0.05$) and Ca^{2+}-time integrals (30°C $1.74 \times 10^{-2} \pm 0.45 \times 10^{-2}$ vs. 37°C $0.87 \times 10^{-2} \pm 0.42 \times 10^{-2}$ ratio units × ms; $P = 0.09$) were higher at 30°C than at 37°C. These particular comparisons must be made cautiously, as although the Ca^{2+} sensitivity of furaptra is largely
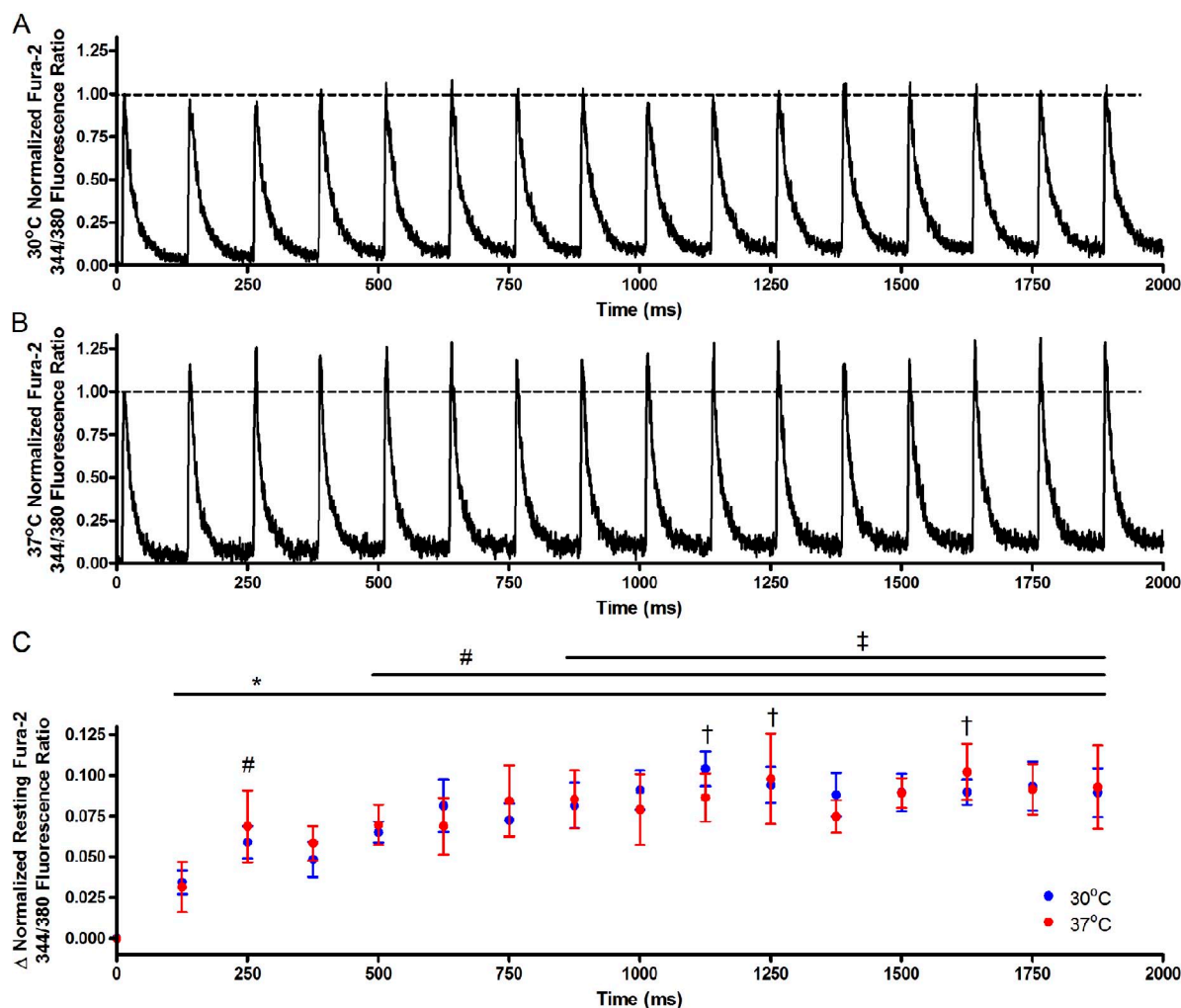
Figure 5. Normalized fura-2 fluorescence recordings during 2 s of 8-Hz stimulation. Mouse lumbrical muscles were loaded with the AM form of the high affinity Ca^{2+}-sensitive indicator fura-2 and subjected to 2 s of 8-Hz stimulation protocol, as described in Materials and methods. Fura-2 ratios are presented normalized to the average ratio during the 20 ms before the first stimulation (0.0) and the peak ratio after the first stimulation (1.0) at both 30 (A) and 37°C (B). The increases in the baseline fura-2 ratio during the protocol at both temperatures are shown in C. Values are mean ± SEM. Two-way split-plot ANOVA analysis revealed no temperature-dependent effects, but several effects caused by repeated stimulation: *, different than 0 ms; #, different than 125 ms; †, different than 250 ms; ‡, different than 375 ms; $P < 0.05$ for all; $n = 4$ per temperature.

temperature independent, its relatively high temperature sensitivity to Mg^{2+} is a potential confounding factor (Konishi et al., 1991). However, when the integration time is reduced to 10 ms poststimulus, the declines in Ca^{2+}-time integral are only significant at 30°C (P < 0.05 vs. P = 0.19 at 37°C), thus supporting the temperature dependence of this effect. These results collectively indicate that the changes in force and force kinetics seen late in the protocol correspond well to changes seen in the ICT.

Analysis of the furaptra ICT records using finer groupings of the first 2 s of the SP protocol, specifically of twitches 1–6, 6–11, and 11–16 (Fig. 4), revealed that relative to unpotentiated levels, the Ca^{2+}-time integral is reduced throughout the 8-Hz stimulation protocol, whereas peak amplitude of the ICT tended to decrease relative to unpotentiated values throughout the protocol, but only reached statistically significant reductions by twitches 6–11 at 30°C and by twitches 11–16 at 37°C.

Fura-2 recordings

Lumbricals loaded with the high affinity Ca^{2+}-sensitive indicator AM-fura-2 demonstrated increases in baseline Ca^{2+}, as summarized in Fig. 5. Importantly, because temperature can affect the fura-2 fluorescence ratio independently of changes in Ca^{2+} (Oliver et al., 2000) and no calibration attempt was made in this study, attempting to directly compare $[Ca^{2+}]_i$ between temperatures is inappropriate; however, relative changes over time are perfectly valid. To facilitate this comparison, the change in fluorescence ratio for each temperature was normalized on a scale of 0–1, with the pre-SP fura-2 ratios at twitch 1 serving as zero (i.e., the unpotentiated baseline cytosolic Ca^{2+} levels) and the peak fluorescence ratio during twitch 1 serving as 1.0. The resulting data demonstrate that the twitch-to-twitch increases in baseline

Ca^{2+} were largest in the first three to four contractions and achieved a plateau by ~1.5 s. The time course of the increase in baseline Ca^{2+} was not influenced by temperature. Fura-2 recordings were only performed for 2 s because of photo-bleaching concerns, as AM-fura-2 loading was much less effective than AM-furaptra loading.

Western blotting results

An additional part of this study was the characterization of the proteins responsible for muscle relaxation in the lumbrical relative to the EDL and soleus muscles, as illustrated in Fig. 6. In general, the expression profile of Ca^{2+}-sequestering proteins of lumbricals lies between the extremes set by the slow-relaxing soleus and fast-relaxing EDL.

DISCUSSION

The primary purpose of this study was to characterize the ICT during SP to determine if the ICT might contribute to the potentiation response seen at physiological temperatures. Although the mouse lumbrical is a relatively unique model with which to study potentiation phenomena, our results reproduce many classic features of SP at 20–37.5°C shown by Krarup (1981) in rat EDL muscle. As a result, our results seem to be generally applicable to both species. As the first study to characterize the ICT during SP in either species, our findings provide novel insights into potential force-modulating mechanisms, which have implications for potentiation of vertebrate striated muscle.

Comparison of force and Ca^{2+} records

Previous work has shown that the mouse lumbrical, despite its fast fiber–type composition, displays no detectable RLC phosphorylation either at rest or after
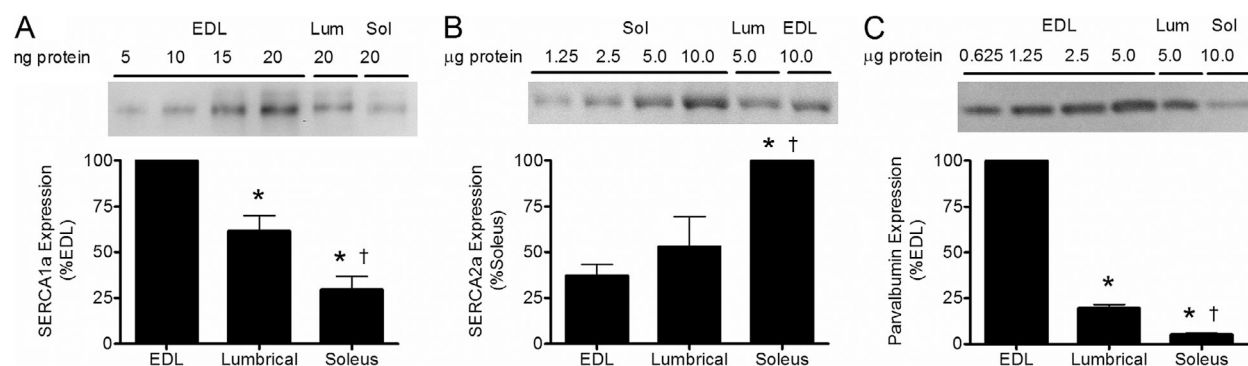
Figure 6. Protein expression of Ca^{2+}-sequestering proteins. This figure depicts sample Western blots and summarized densitometric analysis data for SERCA1a (A), SERCA2a (B), and parvalbumin (C). All values are expressed relative to a linear protein gradient established with either EDL (SERCA1a and parvalbumin) or soleus (Sol; SERCA2a). $n = 8$ for all muscles and proteins. *, significantly different than EDL; †, significantly different than lumbrical (Lum). Significance was taken at P < 0.05. Notes: Two lumbricals from the same animal (one from each hind foot) are pooled, whereas soleus and EDL are not pooled because of size differences. For both SERCA isoforms, each blot had the soleus, EDL, and lumbrical muscle from the same mouse lined up together, with two mice per gel, whereas the parvalbumin blots were run with only one mouse per gel.

stimulation (Smith et al., 2013). Despite this shortcoming, the lumbrical exhibits PTP at 37°C (Smith et al., 2013). In the present study, we have demonstrated that the lumbrical also exhibits SP at 37°C, but not at 30°C (Fig. 3). Additionally, at both temperatures, there are enhancements in the rate of force production during 8-Hz stimulation, indicating a general increase in the apparent Ca^{2+} sensitivity of force production, which does not necessarily translate to elevated peak twitch force (Fig. 3). This may be an effect of elevations in baseline Ca^{2+} that were seen at both temperatures (Fig. 5). We have demonstrated previously a parallel between PTP and elevated Ca^{2+} levels at the onset of stimulation, which may enhance twitch force by enhancing the Ca^{2+} occupancy of troponin C at rest or by reducing competition for troponin C Ca^{2+} binding through saturation of other cytosolic Ca^{2+}-binding proteins such as parvalbumin (Smith et al., 2013), which we show to be present in significant quantities in the lumbrical (Fig. 6). It is also conceivable that elevations in baseline Ca^{2+} could indirectly influence the ICT to enhance or alter subsequent twitch-force development. Redox signaling may also play a role in enhancing Ca^{2+} sensitivity of the contractile proteins. For example, S-glutathionylation of the fast isoform of troponin I can enhance the Ca^{2+} sensitivity of force production (Dutka et al., 2011; Mollica et al., 2012). Whatever the mechanism, it must be both quickly inducible and reversible to account for the potentiation and increases in Ca^{2+} sensitivity seen in this study.

At 37°C, the peak amplitude of the raw furaptra ratios remained unchanged throughout the protocol (Fig. 3 F) despite diminutions in the amplitude of the baseline-adjusted ICT (Fig. 3 G). The maintenance of the amplitude of the raw furaptra ratio is presumably caused by the elevations in baseline Ca^{2+} (Fig. 5). In contrast, both the raw and baseline-adjusted furaptra ratios were depressed from unpotentiated levels at 30°C throughout the 8-Hz stimulation protocol. This may have contributed to the reduced twitch force seen throughout the protocol at this lower temperature. A comparison of the twitch relaxation times and the ICT decay times presents a curious feature of this investigation. Although twitch relaxation parameters were initially hastened by the 8-Hz stimulation, there were no corresponding increases in the decay time of the ICT. In contrast, both ICT and twitch decay times slow beyond ∼2 s of 8-Hz stimulation (Fig. 3). The lack of a general consistency in the pattern of changes in twitch and ICT decay times is a surprising finding, as accelerated relaxation during repeated submaximal contractions has been ascribed to faster cytosolic Ca^{2+} removal (Vøllestad et al., 1997; Tupling, 2009). Our present finding suggests that this may not be the case. Finally, evidence from intact frog skeletal fibers has shown that it is the duration, and not the amplitude, of the ICT that is most important for isometric twitch-force development (Sun et al., 1996);

thus, the slowing of the ICT may have been a force-enhancing factor in SP.

It is clear that the ICT had some influence on the force response, but the extent to which this extends is unknown because of myriad confounding factors including the effects of metabolites and metabolic byproducts, reactive oxygen and nitrogen species, parvalbumin saturation levels, elevated baseline Ca^{2+}, and posttranslational modifications of key proteins. Specific investigation of these aspects and their role in potentiation as modulators of force, the contractile proteins, and cytosolic Ca^{2+} levels is beyond the scope of this investigation. Considerable effort will be required to discern the specific effects of each of these factors on the force response during SP. This area of research will undoubtedly yield fascinating results in the future.

Changes in Ca^{2+} in relation to other studies

Many of the features of the changes in cytosolic Ca^{2+} are consistent with the features of many known physiological phenomena. For example, Hollingworth and Baylor (2013) report that a significant parvalbumin concentration in fast-twitch muscle fibers delays the return of cytosolic Ca^{2+} concentration to resting levels. As the lumbrical contains significant parvalbumin, this may contribute to the elevations in baseline Ca^{2+} seen in this and in our previous investigation on PTP (Smith et al., 2013). Additionally, the declines in baseline-adjusted ICT amplitude seen during SP are consistent with the general properties of Ca^{2+}-dependent inactivation of Ca^{2+} release from the SR seen during closely spaced contractions (Hollingworth et al., 1996; Posterino and Lamb, 2003; Caputo et al., 2004; Barclay, 2012). As the degree of Ca^{2+} inactivation of Ca^{2+} release is generally greater at lower temperatures, the greater reductions in ICT amplitude and area at 30°C than at 37°C are also generally consistent with this property. Finally, the presence of parvalbumin in the lumbrical poses a degree of complexity to the mechanism underlying the prolongation of the ICT we observed in this study. As the Ca^{2+}-binding properties of parvalbumin account for 50–73% of the rate of ICT decay during relaxation of fast-twitch rodent and frog muscle (Hou et al., 1993; Hollingworth et al., 1996; Carroll et al., 1997), an elevation in baseline Ca^{2+} could indirectly slow the rate of decay of the ICT by saturating the Ca^{2+}-buffering capacity of parvalbumin (Hollingworth et al., 1996). However, this mechanism is presently difficult to reconcile in the absence of slowed ICT decay during PTP where baseline Ca^{2+} is similarly elevated (Smith et al., 2013). An equally probable cause of ICT slowing is the accumulation of metabolic byproducts such as ADP and/or P_i, which slow the Ca^{2+}-pumping activities of SERCA, and would accordingly be expected to prolong ICT decay times (Stienen et al., 1993; Macdonald and Stephenson, 2001). Although our data cannot confirm the validity of any of these proposed mechanisms,

it provides a theoretical framework upon which to base further testing.

Limitations

Both Mg^{2+} and Ca^{2+} increase the fluorescence ratio of furaptra; therefore, these results most likely contain contamination from the Mg^{2+} signal at rest, and may contain a progressively increasing Mg^{2+} artifact during the repetitive stimulation protocol (Konishi et al., 1991; Hollingworth et al., 1996). However, because of the low intensity of this protocol, the progressive component of this Mg^{2+} contamination is unlikely to be of significant consequence to the conclusions made in this study. Although it was assumed that the locus of the furaptra was the cytosol, AM dyes are known to compartmentalize forming localized noncytosolic contributions to the universal fluorescence, which may have a confounding effect on the results (see Morgan et al., 1997). Finally, although the ability of furaptra to precisely track the ICT has not been definitively demonstrated for 37°C (Hollingworth et al., 1996), the parallel responses at 30 and 37°C lend ostensible validity to the 37°C data.

Conclusions

The force response to repetitive low frequency stimulation is the result of the balance between mechanisms of force enhancement and force diminishment. Although the force-enhancing effects of myosin RLC phosphorylation and its effects on the Ca^{2+} sensitivity of cross-bridge formation are well documented (Stull et al., 2011), this study has highlighted both parallels and discrepancies between changes in the ICT characteristics and the force response during SP. Not the least of these is our finding that just as in PTP, elevations in baseline Ca^{2+} occur during SP, an effect that is likely to contribute to the potentiation response as a means of increasing the Ca^{2+} sensitivity of force production. Although much work remains to definitively establish any causal links between changes in Ca^{2+} and force responses, the findings in this study provide a basis for further investigations into both Ca^{2+}-based and Ca^{2+}-independent mechanisms and how they specifically influence the characteristics of the force response during repeated stimulation.

REFERENCES

Barclay, C.J. 2012. Quantifying Ca^{2+} release and inactivation of Ca^{2+} release in fast- and slow-twitch muscles. *J. Physiol.* 590:6199–6212. http://dx.doi.org/10.1113/jphysiol.2012.242073

Caputo, C., P. Bolaños, and A. Gonzalez. 2004. Inactivation of Ca^{2+} transients in amphibian and mammalian muscle fibres. *J. Muscle Res. Cell Motil.* 25:315–328. http://dx.doi.org/10.1007/s10974-004-4071-z

Carroll, S.L., M.G. Klein, and M.F. Schneider. 1997. Decay of calcium transients after electrical stimulation in rat fast- and slow-twitch skeletal muscle fibres. *J. Physiol.* 501:573–588. http://dx.doi.org/10.1111/j.1469-7793.1997.573bm.x

Close, R., and J.F.Y. Hoh. 1968. Influence of temperature on isometric contractions of rat skeletal muscles. *Nature.* 217:1179–1180. http://dx.doi.org/10.1038/2171179a0

Dutka, T.L., J.P. Mollica, G.S. Posterino, and G.D. Lamb. 2011. Modulation of contractile apparatus Ca^{2+} sensitivity and disruption of excitation-contraction coupling by S-nitrosoglutathione in rat muscle fibres. *J. Physiol.* 589:2181–2196. http://dx.doi.org/10.1113/jphysiol.2010.200451

Gittings, W., J. Huang, I.C. Smith, J. Quadrilatero, and R. Vandenboom. 2011. The effect of skeletal myosin light chain kinase gene ablation on the fatigability of mouse fast muscle. *J. Muscle Res. Cell Motil.* 31:337–348. http://dx.doi.org/10.1007/s10974-011-9239-8

Hanson, J. 1974. The effects of repetitive stimulation on the action potential and the twitch of rat muscle. *Acta Physiol. Scand.* 90:387–400. http://dx.doi.org/10.1111/j.1748-1716.1974.tb05600.x

Hollingworth, S., and S.M. Baylor. 2013. Return of myoplasmic calcium (Ca) to resting levels following stimulation of fast- and slow-twitch mouse muscle fibers. *Biophys. J.* 104:291a–292a. http://dx.doi.org/10.1016/j.bpj.2012.11.1629

Hollingworth, S., M. Zhao, and S.M. Baylor. 1996. The amplitude and time course of the myoplasmic free $[Ca^{2+}]$ transient in fast-twitch fibers of mouse muscle. *J. Gen. Physiol.* 108:455–469. http://dx.doi.org/10.1085/jgp.108.5.455

Hou, T.T., J.D. Johnson, and J.A. Rall. 1993. Role of parvalbumin in relaxation of frog skeletal muscle. *Adv. Exp. Med. Biol.* 332:141–153. http://dx.doi.org/10.1007/978-1-4615-2872-2_13

Isaacson, A. 1969. Post-staircase potentiation, a long-lasting twitch potentiation of muscles induced by previous activity. *Life Sci.* 8:337–342. http://dx.doi.org/10.1016/0024-3205(69)90225-2

Klug, G.A., B.R. Botterman, and J.T. Stull. 1982. The effect of low frequency stimulation on myosin light chain phosphorylation in skeletal muscle. *J. Biol. Chem.* 257:4688–4690.

Konishi, M., S. Hollingworth, A.B. Harkins, and S.M. Baylor. 1991. Myoplasmic calcium transients in intact frog skeletal muscle fibers monitored with the fluorescent indicator furaptra. *J. Gen. Physiol.* 97:271–301. http://dx.doi.org/10.1085/jgp.97.2.271

Krarup, C. 1981. Temperature dependence of enhancement and diminution of tension evoked by staircase and by tetanus in rat muscle. *J. Physiol.* 311:373–387.

Laemmli, U.K. 1970. Cleavage of structural proteins during the assembly of the head of bacteriophage T4. *Nature.* 227:680–685. http://dx.doi.org/10.1038/227680a0

Macdonald, W.A., and D.G. Stephenson. 2001. Effects of ADP on sarcoplasmic reticulum function in mechanically skinned skeletal muscle fibres of the rat. *J. Physiol.* 532:499–508. http://dx.doi.org/10.1111/j.1469-7793.2001.0499f.x

MacIntosh, B.R., M.J. Smith, and D.E. Rassier. 2008. Staircase but not posttetanic potentiation in rat muscle after spinal cord hemisection. *Muscle Nerve.* 38:1455–1465. http://dx.doi.org/10.1002/mus.21096

Manning, D.R., and J.T. Stull. 1982. Myosin light chain phosphorylation-dephosphorylation in mammalian skeletal muscle. *Am. J. Physiol.* 242:C234–C241.

Metzger, J.M., M.L. Greaser, and R.L. Moss. 1989. Variations in cross-bridge attachment rate and tension with phosphorylation of myosin in mammalian skinned skeletal muscle fibers. Implications for twitch potentiation in intact muscle. *J. Gen. Physiol.* 93:855–883. http://dx.doi.org/10.1085/jgp.93.5.855

Mollica, J.P., T.L. Dutka, T.L. Merry, C.R. Lamboley, G.K. McConell, M.J. McKenna, R.M. Murphy, and G.D. Lamb. 2012. S-glutathionylation of troponin I (fast) increases contractile apparatus Ca^{2+} sensitivity in fast-twitch muscle fibres of rats and humans. *J. Physiol.* 590:1443–1463.

Moore, R.L., B.M. Palmer, S.L. Williams, H. Tanabe, R.W. Grange, and M.E. Houston. 1990. Effect of temperature on myosin phosphorylation in mouse skeletal muscle. *Am. J. Physiol.* 259:C432–C438.

Morgan, D.L., D.R. Claflin, and F.J. Julian. 1997. The relationship between tension and slowly varying intracellular calcium concentration in intact frog skeletal muscle. *J. Physiol.* 500:177–192.

Oliver, A.E., G.A. Baker, R.D. Fugate, F. Tablin, and J.H. Crowe. 2000. Effects of temperature on calcium-sensitive fluorescent probes. *Biophys. J.* 78:2116–2126. http://dx.doi.org/10.1016/S0006-3495(00)76758-0

Persechini, A., J.T. Stull, and R. Cooke. 1985. The effect of myosin phosphorylation on the contractile properties of skinned rabbit skeletal muscle fibers. *J. Biol. Chem.* 260:7951–7954.

Posterino, G.S., and G.D. Lamb. 2003. Effect of sarcoplasmic reticulum Ca^{2+} content on action potential-induced Ca^{2+} release in rat skeletal muscle fibres. *J. Physiol.* 551:219–237. http://dx.doi.org/10.1113/jphysiol.2003.040022

Rassier, D.E., L.A. Tubman, and B.R. MacIntosh. 1999. Staircase in mammalian muscle without light chain phosphorylation. *Braz. J. Med. Biol. Res.* 32:121–129. http://dx.doi.org/10.1590/S0100-879X1999000100018

Ryder, J.W., K.S. Lau, K.E. Kamm, and J.T. Stull. 2007. Enhanced skeletal muscle contraction with myosin light chain phosphorylation by a calmodulin-sensing kinase. *J. Biol. Chem.* 282:20447–20454. http://dx.doi.org/10.1074/jbc.M702927200

Smith, I.C. 2014. The role of cytosolic calcium in potentiation of mouse lumbrical muscle. Doctoral dissertation. University of Waterloo, Waterloo, Ontario. 179 pp.

Smith, I.C., W. Gittings, J. Huang, E.M. McMillan, J. Quadrilatero, A.R. Tupling, and R. Vandenboom. 2013. Potentiation in mouse lumbrical muscle without myosin light chain phosphorylation: Is resting calcium responsible? *J. Gen. Physiol.* 141:297–308. http://dx.doi.org/10.1085/jgp.201210918

Stienen, G.J., I.A. van Graas, and G. Elzinga. 1993. Uptake and caffeine-induced release of calcium in fast muscle fibers of *Xenopus laevis*: effects of MgATP and P$_i$. *Am. J. Physiol.* 265:C650–C657.

Stull, J.T., K.E. Kamm, and R. Vandenboom. 2011. Myosin light chain kinase and the role of myosin light chain phosphorylation in skeletal muscle. *Arch. Biochem. Biophys.* 510:120–128. http://dx.doi.org/10.1016/j.abb.2011.01.017

Sun, Y.B., F. Lou, and K.A.P. Edman. 1996. The relationship between the intracellular Ca^{2+} transient and the isometric twitch force in frog muscle fibres. *Exp. Physiol.* 81:711–724.

Sweeney, H.L., and J.T. Stull. 1990. Alteration of cross-bridge kinetics by myosin light chain phosphorylation in rabbit skeletal muscle: implications for regulation of actin-myosin interaction. *Proc. Natl. Acad. Sci. USA.* 87:414–418. http://dx.doi.org/10.1073/pnas.87.1.414

Tupling, A.R. 2009. The decay phase of Ca^{2+} transients in skeletal muscle: regulation and physiology. *Appl. Physiol. Nutr. Metab.* 34:373–376. http://dx.doi.org/10.1139/H09-033

Vandenboom, R., W. Gittings, I.C. Smith, R.W. Grange, and J.T. Stull. 2013. Myosin phosphorylation and force potentiation in skeletal muscle: evidence from animal models. *J. Muscle Res. Cell Motil.* 34:317–332. http://dx.doi.org/10.1007/s10974-013-9363-8

Vøllestad, N.K., I. Sejersted, and E. Saugen. 1997. Mechanical behavior of skeletal muscle during intermittent voluntary isometric contractions in humans. *J. Appl. Physiol.* 83:1557–1565.

Walker, S.M. 1951. Failure of potentiation in successive, posttetanic, and summated twitches in cooled skeletal muscle of the rat. *Am. J. Physiol.* 166:480–484.

Zhi, G., J.W. Ryder, J. Huang, P. Ding, Y. Chen, Y. Zhao, K.E. Kamm, and J.T. Stull. 2005. Myosin light chain kinase and myosin phosphorylation effect frequency-dependent potentiation of skeletal muscle contraction. *Proc. Natl. Acad. Sci. USA.* 102:17519–17524. http://dx.doi.org/10.1073/pnas.0506846102